Journal of Molecular Liquids 218 (2016) 393–399

Contents lists available at ScienceDirect

Journal of Molecular Liquids

journal homepage: www.elsevier.com/locate/molliq

Free convection of magnetic nanofluid considering MFD viscosity effect

M. Sheikholeslami [a,*], M.M. Rashidi [b,c], T. Hayat [d,e], D.D. Ganji [a]

[a] Department of Mechanical Engineering, Babol University of Technology, Babol, Islamic Republic of Iran
[b] Shanghai Key Lab of Vehicle Aerodynamics and Vehicle Thermal Management Systems, Tongji University, 4800 Cao An Rd., Jiading, Shanghai 201804, China
[c] ENN-Tongji Clean Energy Institute of advanced studies, Shanghai, China
[d] Department of Mathematics, Quaid-I-Azam University 45320, Islamabad 44000, Pakistan
[e] Department of Mathematics, Faculty of Science, King Abdulaziz University, P.O. Box 80257, Jeddah 21589, Saudi Arabia

ARTICLE INFO

Article history:
Received 23 June 2015
Received in revised form 30 December 2015
Accepted 28 February 2016
Available online xxxx

Keywords:
Nanofluid
MHD
CVFEM
MFD
Brownian motion

ABSTRACT

In this study effect of magnetic field dependent (MFD) viscosity on free convection heat transfer of nanofluid in an enclosure is investigated. The bottom wall has constant flux heating element. Single phase nanofluid model is utilized considering Brownian motion. Control Volume based Finite Element Method is applied to simulate this problem. The effects of viscosity parameter, Hartmann number and Rayleigh number on hydrothermal behavior have been examined. Results show that Nusselt number is an increasing function of Rayleigh number and volume fraction of nanoparticle while it is a decreasing function of viscosity parameter and Hartmann number. Also it can be found that reduction of Nusselt number due to MFD viscosity effect are more sensible for high Rayleigh number and low Hartmann number.

Nomenclature

B	Magnetic field
C_p	Specific heat
Gr_f	Grashof number
Ha	Hartmann number $(= LB_x\sqrt{\sigma_f/\mu_f})$
Nu	Nusselt number
Pr	Prandtl number $(=\upsilon_f/\alpha_f)$
T	Fluid temperature
U, V	Dimensionless velocity components in the X-direction and Y-direction
X, Y	Dimensionless space coordinates
k	Thermal conductivity
L	Length of the enclosure
$\vec{g}$	Gravitational acceleration vector
q''	Heat flux
Ra	Rayleigh number $(=g\beta_f q'' L^4/(k\alpha_f\upsilon_f))$

Greek symbols

ω, Ω	Vorticity & dimensionless vorticity
θ_M	Angle of magnetic field
σ	Electrical conductivity
δ^*	Viscosity parameter
α	Thermal diffusivity
ϕ	Volume fraction
μ	Dynamic viscosity
v	Kinematic viscosity
ψ & Ψ	Stream function & dimensionless stream function
Θ	Dimensionless temperature
ρ	Fluid density
β	Thermal expansion coefficient

Subscripts

c	Cold
h	Hot
loc	Local
ave	Average
nf	Nanofluid
f	Base fluid
s	Solid particles

1. Introduction

Magnetohydrodynamic has attracted noteworthy attention due to its numerous applications in petroleum industries and agricultural

* Corresponding author.
E-mail addresses: m_sh_3750@yahoo.com, m.sheikholeslami@stu.nit.ac.ir (M. Sheikholeslami).

http://dx.doi.org/10.1016/j.molliq.2016.02.093
0167-7322/

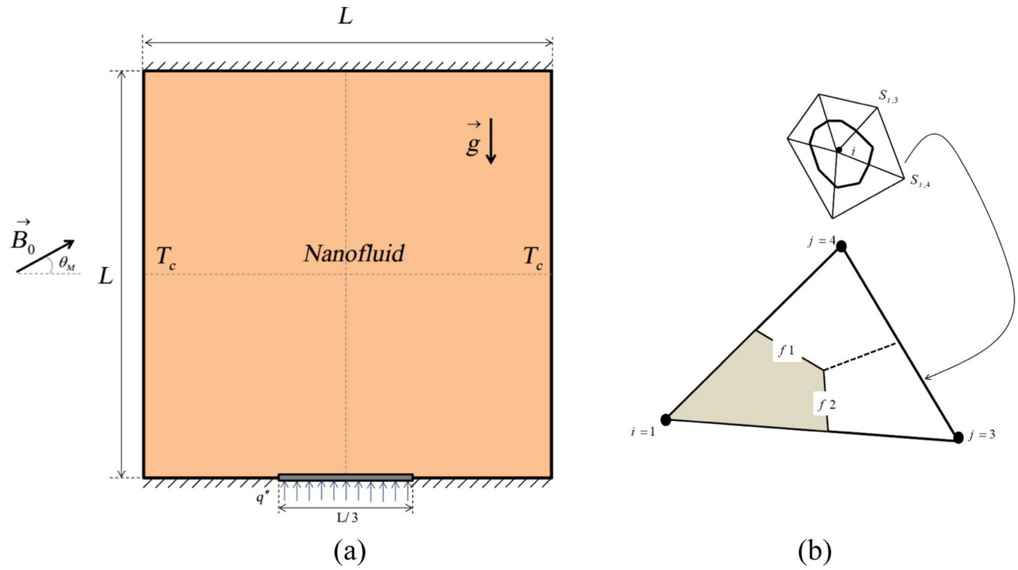

Fig. 1. (a) Geometry and the boundary conditions; (b) a sample triangular element and its corresponding control volume.

engineering. Sheikholeslami et al. [1] used two phase model for simulation of magnetic nanofluid forced convective heat transfer in the presence of variable magnetic field. Rudraiah et al. [2] investigated numerically magnetic field effect on natural convection in a rectangular enclosure. They found that the magnetic field reduces the rate of heat transfer. Hayat et al. [3] investigated the magnetohydrodynamic two-dimensional flow with heat and mass transfer over a stretching sheet in the presence of Joule heating and thermophoresis. Force convective heat transfer of magnetic nanofluid in a lid driven semi annulus enclosure has been investigated by Sheikholeslami et al. [4]. Their results showed that Nusselt number has a direct relationship with Reynolds number, nanoparticle volume fraction while it has reverse relationship with Hartmann number. Ferrofluid heat transfer treatment in the presence of variable magnetic field has been studied by Sheikholeslami and Rashidi [5]. They found that Nusselt number increases by considering magnetic field dependent viscosity. Nanjundappa et al. [6] studied the effect of magnetic field dependent (MFD) viscosity on the onset of ferro convection in a ferrofluid saturated horizontal porous layer. Sheikholeslami et al. [7] investigated the effect of variable magnetic field on force convection heat transfer. Their results indicated that the effects of Kelvin forces are more pronounced for high Reynolds number. Thermal radiation effects on MHD forced convection flow adjacent to a non-isothermal wedge were investigated by Chamkha et al. [8]. They showed that local Nusselt number was predicted to decrease as the thermal radiation parameter increased.

Natural convection heat transfer in partitioned cavity has several applications such as: cooling of electronic components, designing building and solar collectors. Kandaswamy et al. [9] studied the free convective flow arising in a closed square cavity. They showed that heat transfer becomes strengthened when the vertical plate is hotter. Sheikholeslami and Ellahi [10] studied three dimensional mesoscopic simulation of magnetic field effect on natural convection of nanofluid. They found that thermal boundary layer thickness increases with the increase of Lorentz forces. Pal and Mondal [11] have investigated radiation effects on combined convection over a vertical flat plate embedded in a porous medium of variable porosity. Sheikholeslami Kandelousi [12] used KKL correlation for simulation of nanofluid flow and heat transfer in a permeable channel. He found that heat transfer enhancement has direct relationship with Reynolds number when power law index is equal to zero.

Conventional heat transfer fluids, including oil, water, and ethylene glycol mixture are poor heat transfer fluids, since the thermal conductivity of these fluids plays an important role on the heat transfer coefficient between the heat transfer medium and the heat transfer surface. An innovative technique for improving heat transfer by using solid particles in the fluids has been used widely during the last decade. Khanafer et al. [13] seem to be the first who have examined heat transfer performance of nanofluids inside an enclosure taking into account the solid particle dispersion. Ellahi [14] studied the MHD flow of non-Newtonian nanofluid in a pipe. He observed that the MHD parameter decreases the fluid motion. Hakeem et al. [15] studied the magnetic field effect on a steady two dimensional laminar radiative flow of an incompressible viscous water based nanofluid over a stretching/shrinking sheet. They found that the lower branch solution vanishes in the presence of higher magnetic field.

Control Volume based Finite Element Method (CVFEM) is a scheme that uses the advantages of both finite volume and finite element methods for simulation of multi-physics problems in complex geometries [16–17]. Sheikholeslami et al. [18] investigated ferrofluid hydrothermal behavior in the presence of thermal radiation. Sheikholeslami Kandelousi [19] studied the effect of spatially variable magnetic field on ferrofluid flow and heat transfer considering a constant heat flux boundary condition. He found that enhancement in heat transfer decreases with increase of Rayleigh number and Magnetic number but it increases with increase of Hartmann number. Recently several authors used different numerical methods in order to simulate nanofluid flow and heat transfer [20–41].

The main purpose of the present paper is to examine the effect of MFD viscosity on MHD nanofluid flow and heat transfer. CVFEM is used to simulate this problem. New single phase model (Koo-Kleinstreuer-Li) was utilized to simulate nanofluid properties. Effects

Table 1
The coefficient values of $Al_2O_3-Water$ nanofluid [12].

Coefficient values	$Al_2O_3-Water$
a_1	52.813488759
a_2	6.115637295
a_3	0.6955745084
a_4	4.17455552786E-02
a_5	0.176919300241
a_6	−298.19819084
a_7	−34.532716906
a_8	−3.9225289283
a_9	−0.2354329626
a_{10}	−0.999063481

Table 2
Thermo physical properties of water and nanoparticles [12].

	$\rho(kg/m^3)$	$C_p(j/kgk)$	$k(W/m.k)$	$\beta\times10^5(K^{-1})$	$d_p(nm)$	$\sigma(\Omega\cdot m)^{-1}$
water	997.1	4179	0.613	21	–	0.05
Al_2O_3	3970	765	25	0.85	47	1×10^{-10}

of viscosity parameter, Rayleigh number and Hartmann number on the flow and heat transfer characteristics have been examined.

2. Geometry definition and boundary conditions

The geometry of this problem is shown in Fig. 1(a). The heat source is centrally located on the bottom surface and its length L/3. The cooling is achieved by the two vertical walls. The heat source has a constant heat flux q'' while the cooling walls have a constant temperature T_c; all the other surfaces are adiabatic. Also, it is also assumed that the uniform magnetic field ($\vec{B} = B_x\vec{e_x} + B_y\vec{e_y}$) of a constant magnitude $B = \sqrt{B_x^2 + B_y^2}$ is applied, where $\vec{e_x}$ and $\vec{e_y}$ are unit vectors in the Cartesian coordinate system. The orientation of the magnetic field form an angle θ_M with horizontal axis such that $\theta_M = \cot^{-1}(B_x/B_y)$. The electric current J and the electromagnetic force F are defined as $J = \sigma(\vec{V}\times\vec{B})$ and $F = \sigma(\vec{V}\times\vec{B})\times\vec{B}$, respectively.

3. Mathematical modeling and numerical procedure

3.1. Problem formulation

The flow is steady, two-dimensional, laminar and incompressible. The induced electric current and Joule heating are neglected. The magnetic Reynolds number is assumed to be small so that the induced magnetic field can be neglected compared to the applied magnetic field. Neglecting displacement currents, induced magnetic field, and using the Boussinesq approximation, the governing equations of heat transfer and fluid flow for nanofluid can be obtained as follows:

$$\frac{\partial u}{\partial x} + \frac{\partial v}{\partial y} = 0 \tag{1}$$

$$\begin{aligned}\rho_{nf}\left(u\frac{\partial u}{\partial x} + v\frac{\partial u}{\partial y}\right) &= -\frac{\partial P}{\partial x} + \eta\left(\frac{\partial^2 u}{\partial x^2} + \frac{\partial^2 u}{\partial y^2}\right) \\ &\quad + \sigma_{nf}{B_0}^2\left(v\sin\theta_M\cos\theta_M - u\sin^2\theta_M\right)\end{aligned} \tag{2}$$

$$\begin{aligned}\rho_{nf}\left(u\frac{\partial v}{\partial x} + v\frac{\partial v}{\partial y}\right) &= -\frac{\partial P}{\partial y} + \eta\left(\frac{\partial^2 v}{\partial x^2} + \frac{\partial^2 v}{\partial y^2}\right) + \rho_{nf}\beta_{nf}g(T - T_c) \\ &\quad + \sigma_{nf}{B_0}^2(u\sin\theta_M\cos\theta_M - v\cos^2\theta_M)\end{aligned} \tag{3}$$

$$u\frac{\partial T}{\partial x} + v\frac{\partial T}{\partial y} = \alpha_{nf}\left(\frac{\partial^2 T}{\partial x^2} + \frac{\partial^2 T}{\partial y^2}\right) \tag{4}$$

where $\eta = (1 + \vec{\delta}.\vec{B})\mu_{nf}$, the variation of MFD viscosity (δ) has been taken to be isotropic, $\delta_1 = \delta_2 = \delta_3 = \delta$. The effective density (ρ_{nf}), the thermal expansion coefficient (β_{nf}), heat capacitance $(\rho C_p)_{nf}$ and electrical conductivity of nanofluid (σ_{nf}) of the nanofluid are defined as [12]:

Table 3
Comparison of the average Nusselt number Nu_{ave} for different grid resolutions at $Ra = 10^5$, $\phi = 0.04$, $\delta^* = 1$, $Ha = 60$ and $\Pr = 6.2$.

Mesh size	81×81	91×91	101×101	111×111	121×121
Nu_{ave}	2.041	2.053	2.065	2.067	2.071

Table 4
Average Nusselt number versus at different Grashof number under various strengths of the magnetic field at $Pr = 0.733$.

Ha	$Gr = 2\times10^4$		$Gr = 2\times10^5$	
	Present	Rudraiah et al. [2]	Present	Rudraiah et al. [2]
0	2.5665	2.5188	5.093205	4.9198
10	2.26626	2.2234	4.9047	4.8053
50	1.09954	1.0856	2.67911	2.8442
100	1.02218	1.011	1.46048	1.4317

$$\begin{aligned}\rho_{nf} &= \rho_f(1-\phi) + \rho_s\phi \\ \beta_{nf} &= \beta_f(1-\phi) + \beta_s\phi \\ (\rho C_p)_{nf} &= (\rho C_p)_f(1-\phi) + (\rho C_p)_s\phi\end{aligned} \tag{5}$$

$$\frac{\sigma_{nf}}{\sigma_f} = 1 + \frac{3(\sigma_s/\sigma_f - 1)\phi}{(\sigma_s/\sigma_f + 2) - (\sigma_s/\sigma_f - 1)\phi}. \tag{6}$$

Koo-Kleinstreuer-Li (KKL) is used to simulate thermal conductivity of nanofluid [12]:

$$k_{\text{eff}} = k_{\text{static}} + k_{\text{Brownian}} \tag{7}$$

$$\frac{k_{\text{static}}}{k_f} = 1 + \frac{3(k_p/k_f - 1)\phi}{(k_p/k_f + 2) - (k_p/k_f - 1)\phi} \tag{8}$$

$$k_{\text{Brownian}} = 5\times10^4\phi\rho_f c_{p,f}\sqrt{\frac{\kappa_b T}{\rho_p d_p}}g'(T, \phi, d_p) \tag{9}$$

$$R_f + \frac{d_p}{k_p} = \frac{d_p}{k_{p,eff}}, R_f = 4\times10^{-8}km^2/W \tag{10}$$

$$\begin{aligned}g'(T, \phi, d_p) &= \left(a_1 + a_2\ln(d_p) + a_3\ln(\phi) + a_4\ln(\phi)\ln(d_p) + a_5\ln(d_p)^2\right)\ln(T) \\ &\quad + \left(a_6 + a_7\ln(d_p) + a_8\ln(\phi) + a_9\ln(\phi)\ln(d_p) + a_{10}\ln(d_p)^2\right)\end{aligned} \tag{11}$$

with the coefficients ai ($i = 0.10$) are based on the type of nanopartices, Al_2O_3-water nanofluids have an R^2 of 98%, respectively [12] (Table 1).

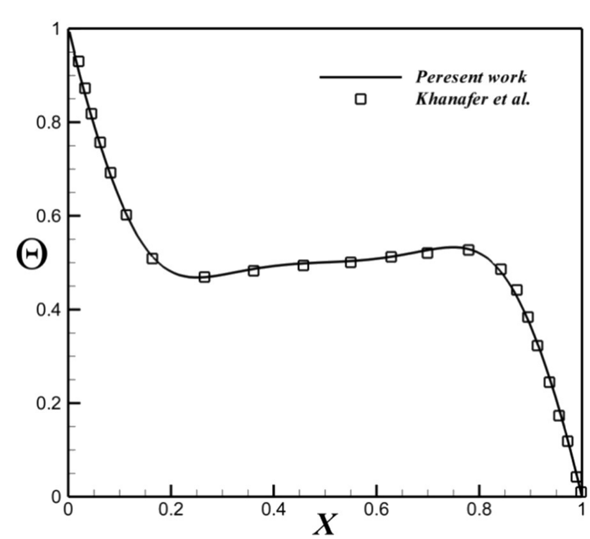

Fig. 2. Comparison of average Nusselt number between the present results and numerical results by Khanafer et al. [13] $Gr = 10^4$, $\phi = 0.1$ and $\Pr = 6.2$ $(Cu - Water)$;

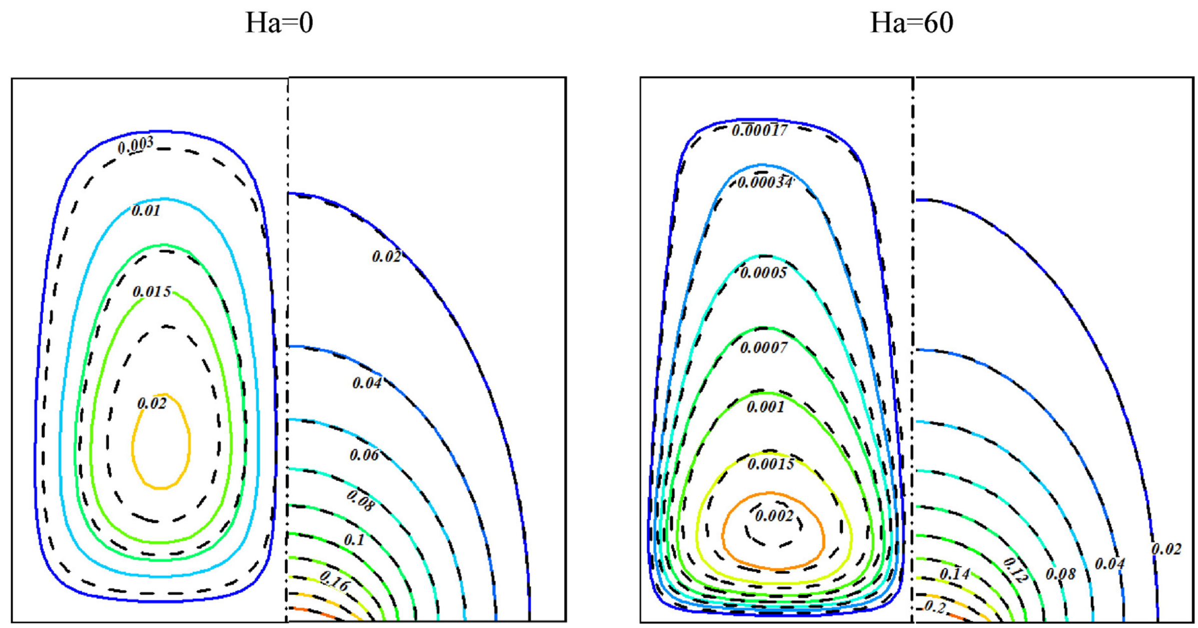

Fig. 3. Effects of viscosity parameter ($\delta^*=1$ (— — —) and $\delta^*=0$ (––)) and Hartmann number on isotherms (right) and streamlines (left) when $\phi=0.04, Ra=10^3$.

The effective viscosity due to micromixing in suspensions, can be obtained as follows [12]:

$$\mu_{\text{eff}} = \mu_{\text{static}} + \mu_{\text{Brownian}} = \mu_{\text{static}} + \frac{k_{\text{Brownian}}}{k_f} \times \frac{\mu_f}{\text{Pr}_f} \tag{12}$$

where $\mu_{\text{static}} = \frac{\mu_f}{(1-\phi)^{2.5}}$ is viscosity of the nanofluid, as given originally by Brinkman.

The stream function and vorticity are defined as:

$$u = \frac{\partial \psi}{\partial y}, v = -\frac{\partial \psi}{\partial x}, \omega = \frac{\partial v}{\partial x} - \frac{\partial u}{\partial y} \tag{13}$$

The stream function satisfies the continuity Eq. (1). The vorticity equation is obtained by eliminating the pressure between the two momentum equations, i.e. by taking y-derivative of Eq. (2) and subtracting from it the x-derivative of Eq. (3). This gives:

$$\begin{aligned} \frac{\partial \psi}{\partial y}\frac{\partial \omega}{\partial x} - \frac{\partial \psi}{\partial x}\frac{\partial \omega}{\partial y} &= \upsilon_{nf}(1+\delta B_0(\cos\theta_M + \sin\theta_M))\left(\frac{\partial^2 \omega}{\partial x^2} + \frac{\partial^2 \omega}{\partial y^2}\right) + \beta_{nf} g\left(\frac{\partial T}{\partial x}\right) \\ &+ \frac{\sigma_{nf} {B_0}^2}{\rho_{nf}}\left(\begin{array}{l} -\frac{\delta v}{\delta y}\sin\theta_M\cos\theta_M + \frac{\delta u}{\delta y}\sin^2\theta_M \\ +\frac{\delta u}{\delta x}\sin\theta_M\cos\theta_M - \frac{\delta v}{\delta x}\cos^2\theta_M \end{array}\right) \end{aligned} \tag{14}$$

$$\frac{\partial \psi}{\partial y}\frac{\partial T}{\partial x} - \frac{\partial \psi}{\partial x}\frac{\partial T}{\partial y} = \alpha_{nf}\left(\frac{\partial^2 T}{\partial x^2} + \frac{\partial^2 T}{\partial y^2}\right) \tag{15}$$

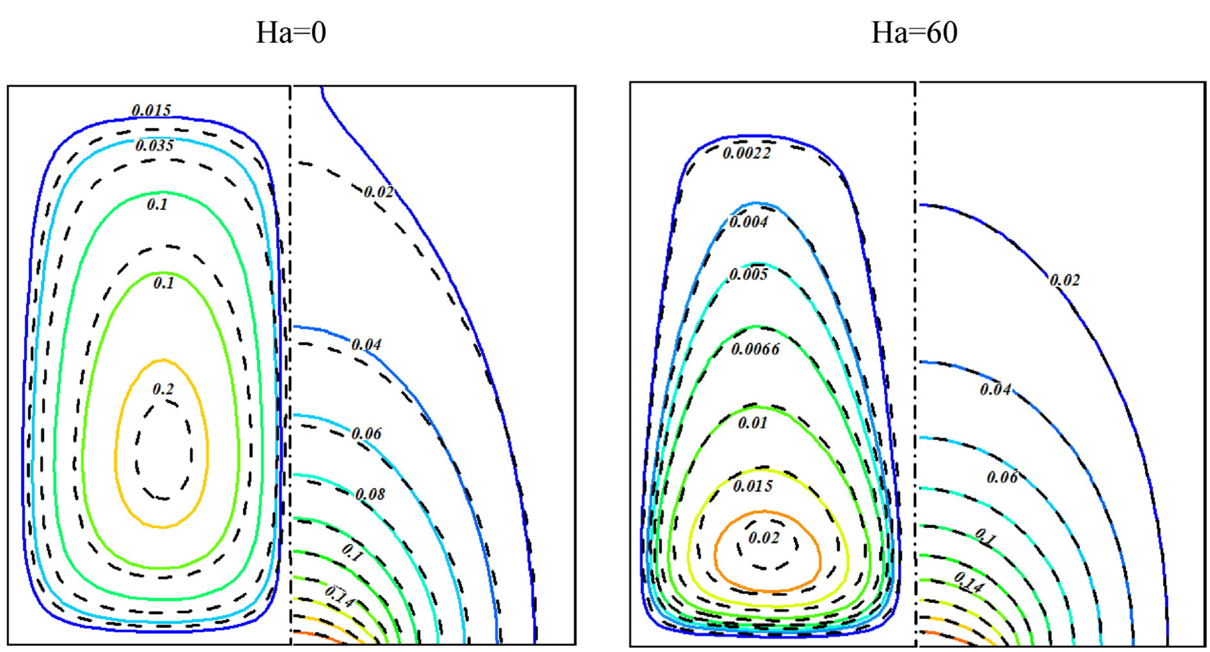

Fig. 4. Effects of viscosity parameter ($\delta^*=1$ (— — —) and $\delta^*=0$ (––)) and Hartmann number on isotherms (right) and streamlines (left) when $\phi=0.04, Ra=10^4$.

$$\frac{\partial^2\psi}{\partial x^2}+\frac{\partial^2\psi}{\partial y^2}=-\omega \tag{16}$$

by introducing the following non-dimensional variables:

$$X=\frac{x}{L},Y=\frac{y}{L},\Omega=\frac{\omega L^2}{\alpha_f},\Psi=\frac{\psi}{\alpha_f},\Theta=\frac{T-T_c}{(q''L/k_f)},U=\frac{uL}{\alpha_f},V=\frac{vL}{\alpha_f} \tag{17}$$

using the dimensionless parameters, the equations now become:

$$\begin{aligned}&\frac{\partial\Psi}{\partial Y}\frac{\partial\Omega}{\partial X}-\frac{\partial\Psi}{\partial X}\frac{\partial\Omega}{\partial Y}=\\&\Pr_f\left(\frac{\mu_{nf}}{\mu_f}\frac{\rho_f}{\rho_{nf}}\frac{k_f}{k_{nf}}\frac{(\rho C_p)_{nf}}{(\rho C_p)_f}\right)(1+\delta^*(\cos\theta_M+\sin\theta_M))\left(\frac{\partial^2\Omega}{\partial X^2}+\frac{\partial^2\Omega}{\partial Y^2}\right)\\&\quad+Ra_f\Pr_f\frac{\beta_{nf}}{\beta_f}\left(\frac{\partial\Theta}{\partial X}\right)\\&\quad+Ha^2\Pr_f\frac{\sigma_{nf}}{\sigma_f}\frac{\rho_f}{\rho_{nf}}\left(-\frac{\delta V}{\delta Y}\tan\theta_M+\frac{\delta U}{\delta Y}\tan^2\theta_M+\frac{\delta U}{\delta X}\tan\theta_M-\frac{\delta V}{\delta X}\right)\end{aligned} \tag{18}$$

$$\frac{\partial\Psi}{\partial Y}\frac{\partial\Theta}{\partial X}-\frac{\partial\Psi}{\partial X}\frac{\partial\Theta}{\partial Y}=\frac{k_{nf}}{k_f}\frac{(\rho C_p)_f}{(\rho C_p)_{nf}}\left(\frac{\partial^2\Theta}{\partial X^2}\right) \tag{19}$$

$$\frac{\partial^2\Psi}{\partial X^2}+\frac{\partial^2\Psi}{\partial Y^2}=-\Omega \tag{20}$$

where $Ra_f=g\beta_f L^4 q''/(k_f\alpha_f\upsilon_f)$ is the Rayleigh number for the base fluid, $Ha=LB_x\sqrt{\sigma_f/\mu_f}$ is the Hartmann number and $\Pr_f=\upsilon_f/\alpha_f$ is the Prandtl number for the base fluid. Also $\delta^*=\delta B_0$ is the viscosity parameter. The thermo physical properties of the nanofluid are given in Table 2 [12]. The boundary conditions as shown in Fig. 1 are:

$$\begin{array}{ll}\partial\Theta/\partial n=-1.0 & \text{on the heat source}\\ \Theta=0.0 & \text{on the left and right}\\ \partial\Theta/\partial n=0.0 & \text{on all the other adiabatic surfaces}\\ \Psi=0.0 & \text{on all solid boundaries.}\end{array} \tag{21}$$

The values of vorticity on the boundary of the enclosure can be obtained using the stream function formulation and the known velocity conditions during the iterative solution procedure. The local Nusselt number of the nanofluid along the heat source can be expressed as:

$$Nu_{local}=\left(\frac{k_{nf}}{k_f}\right)\frac{1}{\theta}\bigg|_{L/3<X<2L/3,Y=0}. \tag{22}$$

The average Nusselt number is evaluated as:

$$Nu_{ave}=\frac{1}{L/3}\int_{L/3}^{2L/3}Nu_{loc}(X)dX. \tag{23}$$

Nusselt ratio is defined as follows:

$$Nu_{ratio}=\frac{Nu_{ave}|_{\delta^*=1}}{Nu_{ave}|_{\delta^*=0}}. \tag{24}$$

3.2. Numerical procedure

The Control Volume based Finite Element Method is used in this work. The building block of the discretization is the triangular element and the values of variables are approximated with linear interpolation within the elements. The control volumes are created by joining the center of each element in the support to the mid points of the element sides that pass through the central node *i* which creates a close polygonal control volume (see Fig. 1(b)). The set of governing equations is integrated over the Control Volume with the use of linear interpolation inside the finite element and the obtained algebraic equations are solved by the Gauss–Seidel Method. A FORTRAN code is developed to solve the present problem using a structured mesh of linear triangular. The details of this method are mentioned in [16].

4. Grid testing and code validation

To assure the grid-independency of the present solution a mesh testing procedure was conducted. Different mesh combinations were explored for the case of $Ra=10^5$, $\phi=0.04$, $\delta^*=0.03$, $Ha=60$ and $\Pr=6.2$ as shown in Table 3. The present code was tested for grid independence by calculating the average Nusselt number on hot bottom

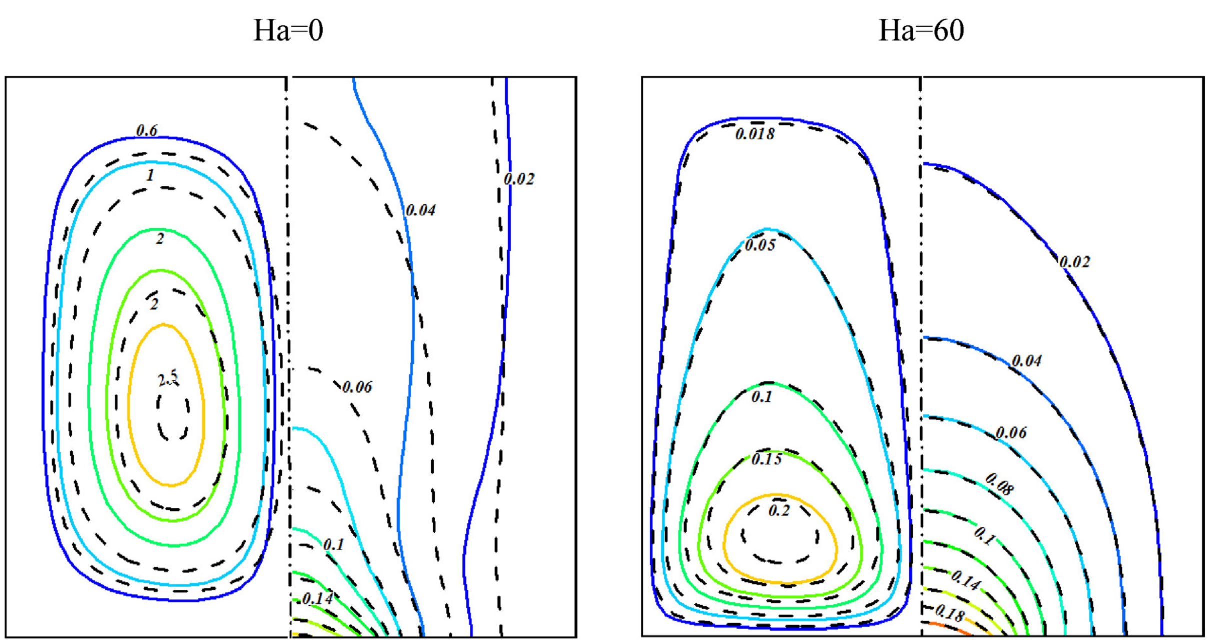

Fig. 5. Effects of viscosity parameter ($\delta^*=1$ (— — —) and $\delta^*=0$ (—)) and Hartmann number on isotherms (right) and streamlines (left) when $\phi=0.04, Ra=10^5$.

wall. In harmony with this, it was found that a grid size of 101×101 ensures a grid-independent solution. The convergence criterion for the termination of all computations is:

$$\max_{\mathrm{grid}}\left|\Gamma^{s+1}-\Gamma^{s}\right|\leq 10^{-7} \tag{25}$$

where s is the iteration number and Γ stands for the independent variables (Ω,Ψ,Θ). The average Nusselt number using different Gr and Ha numbers has been compared with those obtained by Rudraiah et al. [2] as shown in Table 4. In Fig. 2, the present computation is validated against the results of Khanafer et al. [13] carried for natural convection in an enclosure filled with Cu–water nanofluid. These comparisons prove an excellent agreement between the present calculations and the previous works.

5. Results and discussion

In this study magnetohydrodynamic natural convective heat transfer in a cooling system of electronic components is investigated. Magnetic field dependent (MFD) viscosity effect is taken in to account. Brownian motion effect is considered for simulating effective thermal conductivity and viscosity. Influence of active parameters such as: Rayleigh number ($Ra = 10^3, 10^4$ and 10^5), Hartmann number ($Ha = 0, 15, 30$ and 60) and viscosity parameter ($\delta^* = 0$, 1) on flow and heat transfer is examined when $\phi = 0.04$, $\Pr = 6.2$.

Effects of viscosity parameter, Hartmann number and Rayleigh number on isotherms and streamlines are shown in Figs. 3, 4 and 5. At low Rayleigh number, the streamlines take the enclosure geometry. By increasing Rayleigh number the prominent heat transfer mechanism is turn from conduction to convection. When the magnetic field is imposed on the enclosure, the velocity field suppressed owing to the retarding effect of the Lorenz force. So intensity of convection weakens significantly. The decelerating effect of the magnetic field is observed from the maximum stream function value. The core vortex is shift downward vertically as the Hartmann number increases. Also imposing magnetic field leads to omit the thermal plume over the bottom wall. At high Hartmann number the conduction heat transfer mechanism is more pronounced. For this reason the isotherms are parallel to each other. Considering MFD viscosity effect increases the thermal boundary

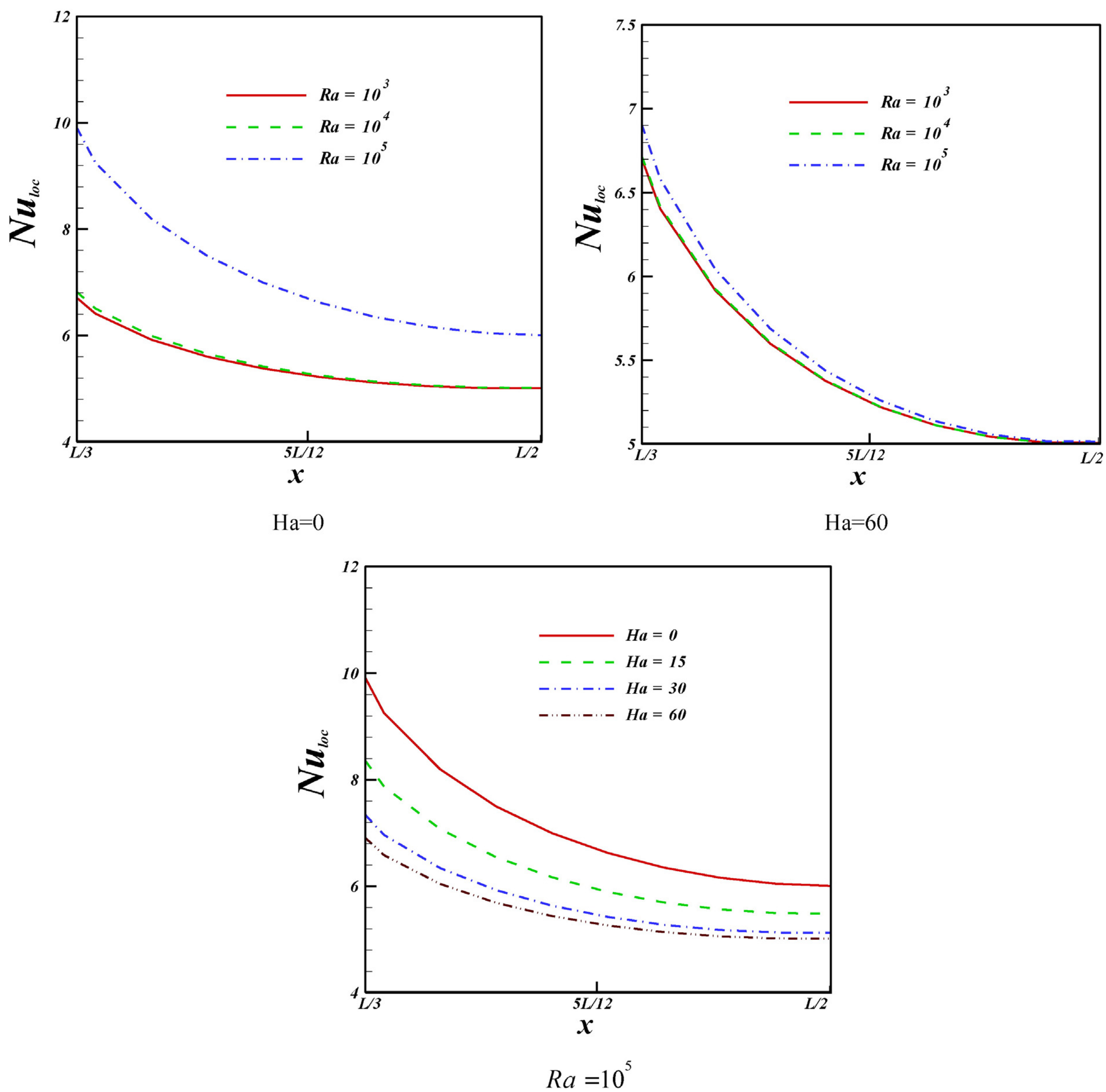

Fig. 6. Effects of Hartmann number and Rayleigh number on local Nusselt number when $\phi = 0.04, \delta^* = 1$, $\Pr = 6.2$.

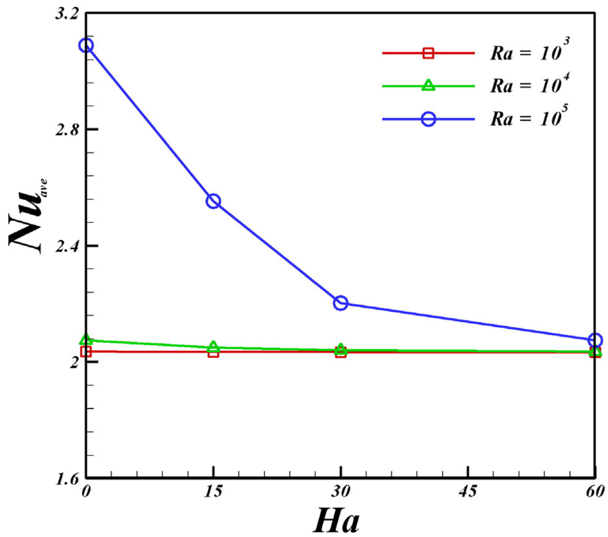

Fig. 7. Effects of Hartmann number and Rayleigh number on average Nusselt number when $\phi = 0.04, \delta^* = 1$, $\Pr = 6.2$.

layer thickness and in turn Nusselt number decreases with increase of viscosity parameter. Also it can be seen that flow circulation increases with increase of this parameter.

Effects of Hartmann number and Rayleigh number on local and average Nusselt number are shown in Figs. 6 and 7. Increasing Rayleigh number leads the Nusselt number to enhance. Increasing Lorentz forces makes the thermal boundary layer thickness to increase and in turn Nusselt number decreases with enhance of Hartmann number. Fig. 8 depicts the effect of Hartmann number and Rayleigh number on Nusselt number ratio. As viscosity parameter increases the rate of heat transfer decreases. This reduction is more pronounced for higher values of Rayleigh number and lower values of Hartmann number. It is an interesting observation that increasing Lorentz forces increases the effect of MFD viscosity of Nusselt number. At low Rayleigh number, considering MFD viscosity has no significant effect on Nusselt number.

6. Conclusions

MFD viscosity effect on magnetohydrodynamic nanofluid hydrothermal behavior is investigated numerically using the Control Volume

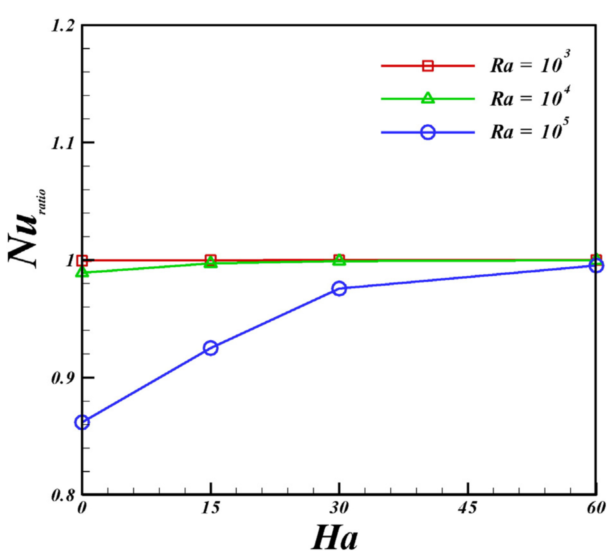

Fig. 8. Effects of Hartmann number and Rayleigh number on Nusselt number ratio when $\phi = 0.04$, $\Pr = 6.2$.

based Finite Element Method. The bottom wall has constant flux heating element. Brownian motion is taken in to accountant in nanofluid model. This geometry can be considered as a system for the cooling of electronic components. Results indicate that Nusselt number increases with enhance of Rayleigh number and volume fraction of nanoparticle while it decreases with increase of viscosity parameter and Hartmann number. Also it can be concluded that reduction in heat transfer due to MFD viscosity is an increasing function of Rayleigh number but it is a decreasing function of Hartmann number.

References

[1] M. Sheikholeslami, M.M. Rashidi, D.D. Ganji, J. Mol. Liq. 212 (2015) 117–126.
[2] N. Rudraiah, R.M. Barron, M. Venkatachalappa, C.K. Subbaraya, Int. J. Eng. Sci. 33 (8) (1995) 1075–1084.
[3] T. Hayat, M. Qasim, Int. J. Heat Mass Transf. 53 (21−22) (2010) 4780–4788.
[4] M. Sheikholeslami, M.M. Rashidi, D.D. Ganji, Comput. Methods Appl. Mech. Eng. 294 (2015) 299–312.
[5] M. Sheikholeslami, M.M. Rashidi, Eur. Phys. J. Plus 130 (2015) 115.
[6] C.E. Nanjundappa, I.S. Shivakumara, M. Ravisha, Int. Commun. Heat Mass Transfer 37 (2010) 1246–1250.
[7] Mohsen Sheikholeslami, Kuppalapalle Vajravelu, Mohammad Mehdi Rashidi, Int. J. Heat Mass Transf. 92 (2016) 339–348.
[8] A.J. Chamkha, M. Mujtaba, A. Quadri, C. Issa, Heat Mass Transf. 39 (2003) 305–312.
[9] Kandaswamy, A.K. Abdul Hakeem, S. Saravanan, Comput. Fluids 111 (16) (April 2015) 179–186.
[10] M. Sheikholeslami, R. Ellahi, Int. J. Heat Mass Transf. 89 (2015) 799–808.
[11] D. Pal, H. Mondal, Meccanica 44 (2009) 133–144.
[12] Mohsen Sheikholeslami Kandelousi, Phys. Lett. A 378 (45) (2014) 3331–3339.
[13] K. Khanafer, K. Vafai, M. Lightstone, Int. J. Heat Mass Transf. 46 (19) (2003) 3639–3653.
[14] R. Ellahi, Appl. Math. Model. 37 (3) (2013) 1451–1467.
[15] A.K. Abdul Hakeem, N. Vishnu Ganesh, B. Ganga, J. Magn. Magn. Mater. 381 (1) (May 2015) 243–257.
[16] Mohsen Sheikholeslami, Davood Domairry Ganji, Academic Press, Print Book, 2015, ISBN 9780128029503 1–226.
[17] Voller VR. World Scientific Publishing *Co*. Pte. Ltd. 5 Tohccxxvc; 2009.
[18] Mohsen Sheikholeslami, Davood Domiri Ganji, Mohammad Mehdi Rashidi, J. Taiwan Inst. Chem. Eng. 47 (2015) 6–17.
[19] Mohsen Sheikholeslami Kandelousi, Eur. Phys. J. B Plus (2014) 129–248.
[20] M. Sheikholeslami, T. Hayat, A. Alsaedi, International Journal of Heat and Mass Transfer 96 (2016) 513–524.
[21] G.H.R. Kefayati, J. Taiwan Inst. Chem. Eng. 54 (2015) 1–10.
[22] M. Sheikholeslami, M. Hatami, D.D. Ganji, J. Mol. Liq. 211 (2015) 577–583.
[23] M.M. Rahman, Hakan F. Öztop, Michael Steele, A.G. Naim, Khaled Al-Salem, Talaat A. Ibrahim, Int. Commun. Heat Mass Transfer 64 (2015) 50–60.
[24] M. Sheikholeslami, H.R. Ashorynejad, P. Rana, Journal of Molecular Liquids 214 (2016) 86–95.
[25] M. Sheikholeslami, Soheil Soleimani, D.D. Ganji, Journal of Molecular Liquids 213 (2016) 153–161.
[26] Kalidas Das, Pinaki Ranjan Duari, Prabir Kumar Kundu, Alex. Eng. J. 53 (2014) 737–745.
[27] Mohsen Sheikholeslami, Shirley Abelman, IEEE Trans. Nanotechnol. 14 (3) (2015) 561–569.
[28] M. Sheikholeslami, J. Braz. Soc. Mech. Sci. Eng. 37 (2015) 1623–1633.
[29] Mohsen Sheikholeslami, Davood Domiri Ganji, Energy 75 (2014) 400–410.
[30] Kalidas Das, J. Egypt. Math. Soc. 23 (2015) 451–456.
[31] Mohsen Sheikholeslami, Mohammad Mehdi Rashidi, Journal of the Taiwan Institute of Chemical Engineers 56 (2015) 6–15.
[32] Kalidas Das, Int. J. Heat Mass Transf. 55 (2012) 7166–7174.
[33] M. Sheikholeslami, D.D. Ganji, Powder Technol. 235 (2013) 873–879.
[34] Hamid Reza Ashorynejad, Abdulmajeed A. Mohamad, Mohsen Sheikholeslami, Int. J. Therm. Sci. 64 (2013) 240–250.
[35] A.K. Abdul Hakeem, R. Kalaivanan, N. Vishnu Ganesh, B. Ganga, Ain Shams Eng. J. 5 (2014) 913–922.
[36] Mohsen Sheikholeslami, Mofid Gorji-Bandpy, Davood Domiri Ganji, Renew. Sust. Energ. Rev. 49 (2015) 444–469.
[37] Junaid Ahmad Khan, M. Mustafa, T. Hayat, M. Sheikholeslami, A. Alsaedi, PLoS ONE 10(3): e0116603. http://dx.doi.org/10.1371/journal.pone.0116603.
[38] Mohsen Sheikholeslami, Davood Domiri Ganji, Physica A 417 (2015) 273–286.
[39] Mohsen Sheikholeslami, Davood Domiri Ganji, M. Younus Javed, R. Ellahi, Journal of Magnetism and Magnetic Materials 374 (2015) 36–43.
[40] Mohsen Sheikholeslami, Davood Domiri Ganji, Comput. Methods Appl. Mech. Engrg. 283 (2015) 651–663.
[41] M. Sheikholeslami, R. Ellahi, Mohsan Hassan, Soheil Soleimani, International Journal of Numerical Methods for Heat & Fluid Flow 24 (8) (2014) 1906–1927.